Regulation of synapse composition by protein acetylation: the role of acetylated cortactin

Tatiana Catarino[1,2], Luís Ribeiro[1,2,*], Sandra D. Santos[1,2,*] and Ana Luísa Carvalho[1,2,‡]

[1]CNC-Center for Neuroscience and Cell Biology, University of Coimbra, Coimbra, 3004-517, Portugal
[2]Department of Life Sciences, University of Coimbra, Coimbra, 3004-517, Portugal

*These authors contributed equally to this work
‡Author for correspondence (alc@cnc.uc.pt)

Accepted 3 September 2012
Journal of Cell Science 126, 149–162

doi: 10.1242/jcs.110742

Summary

Protein acetylation affects synaptic plasticity and memory, but its effects on synapse composition have not been addressed. We found that protein acetylation promotes the dendritic clustering of the excitatory postsynaptic scaffold protein PSD95 in hippocampal neurons, without affecting the total levels of this protein. Cortactin, an F-actin-binding protein enriched in dendritic spines, is a substrate for acetylation and has a role in spine morphogenesis. Recent studies showed that cortactin acetylation changes its ability to bind F-actin and regulates cellular motility, but the function of cortactin acetylation in neuronal cells is so far unknown. We tested whether acetylation of cortactin influences its morphogenic function by overexpressing wild-type cortactin, or the mimetic mutants for acetylated or deacetylated cortactin, in hippocampal neurons, and found that cortactin acetylation has an impact on PSD95 clustering, independent from its function as actin dynamics regulator. Moreover, acetylated cortactin can rescue the reduction in PSD95 clustering mediated by knockdown of cortactin. We also found that acetylation of cortactin is correlated with decreased cortactin interaction with p140Cap and Shank1, and with lower cortactin phosphorylation at tyrosine 421. The neurotrophin BDNF promoted the acetylation of cortactin in hippocampal neurons, suggesting that BDNF may regulate excitatory synapses and PSD95 dendritic clustering at least in part by changing the acetylation level of cortactin. Our findings unravel an unsuspected role for cortactin acetylation in the regulation of PSD95 dendritic clustering, which may work in concert with cortactin's role in spine development.

Key words: Cortactin, Acetylation, PSD95, Excitatory synapses

Introduction

The critical role of phosphorylation in synaptic plasticity and memory has been established using a variety of different model systems. More recently, protein acetylation has also been attributed an important role in these processes (Sharma, 2010). Learning and memory in wild-type mice as well as in mouse models of neurodegeneration is facilitated by increased histone-tail acetylation induced by histone deacetylases inhibitors. In addition to histones, acetylation of other proteins may also be important for memory formation. In fact, several other proteins including transcription factors, transport proteins, α-tubulin and acetyltransferases are acetylated proteins (Kouzarides, 2000; Spange et al., 2009; Yang and Seto, 2008). Therefore, it is to be expected that changes in the acetylation status of other proteins, in addition to histones, may potentially be involved in the facilitatory effects of deacetylase inhibition in synaptic plasticity and memory. In *Drosophila* neurons, elongator protein 3 (ELP3) was found to acetylate the active zone ELKS family member Bruchpilot, and *elp3* mutants show morphological defects in active zones, resulting in a larger pool of synaptic vesicles ready for immediate release (Miśkiewicz et al., 2011). Despite the evidences indicating a role for protein acetylation in synapse number (Guan et al., 2009), synaptic plasticity and memory (Chwang et al., 2007; Fischer et al., 2007; Fontán-Lozano et al., 2008; Guan et al., 2009; Kim et al., 2012; Levenson et al., 2004; Miller et al., 2008; Stefanko et al., 2009; Vecsey et al., 2007; Yeh et al., 2004), the impact of protein acetylation on the molecular composition of synapses has never been addressed.

Cortactin is highly enriched in spines where it colocalizes with F-actin (Hering and Sheng, 2003; Racz and Weinberg, 2004), and has recently been described as a target for acetylation (Zhang et al., 2007). Cortactin is a substrate for HDAC6 and for the acetyl-transferase p300-CBP-associated factor (Zhang et al., 2009), and cortactin acetylation prevents cortactin binding to F-actin, resulting in decreased cancer cell migration (Zhang et al., 2007). Cortactin is also a central player in a number of neuron-specific functions including dendritic spine morphogenesis, as supported by the findings that its downregulation results in spine depletion, whereas its overexpression causes spine elongation (Hering and Sheng, 2003). Furthermore, cortactin distribution is dynamically regulated by neuronal activity. Overstimulation of NMDA receptors in hippocampal neurons removed cortactin from dendritic spines (Hering and Sheng, 2003; Iki et al., 2005), and LTP in hippocampal slices was associated with a decrease in synapse-associated cortactin (Seese et al., 2012).

Here we found that protein acetylation, enhanced by HDACs inhibitors, can change the postsynaptic clustering of the scaffold proteins PSD95 and Shank1, as well as the synaptic localization of p140Cap and cortactin, in cultured rat hippocampal neurons. We also showed that neuronal cortactin is regulated by acetylation, which promotes redistribution of cortactin from spines to dendritic shafts and to the cell body. Focusing on how

Journal of Cell Science

cortactin acetylation regulates the clustering of PSD95 in the dendrites of cultured hippocampal neurons we found that overexpression of a mutant of cortactin mimicking the deacetylated protein decreases PSD95 clustering, whereas the mutant that mimics the acetylated form can rescue the decrease in PSD95 clustering mediated by knockdown of cortactin. Furthermore, we addressed the effects of cortactin acetylation on its tyrosine phosphorylation, as well as on its interactions with synaptic binding partners. Finally, we showed that BDNF, which promotes an increase on PSD95 in dendritic spines (Yoshii and Constantine-Paton, 2007), increases the acetylation levels of cortactin. Our data support a function for cortactin acetylation in the regulation of the dendritic clustering of PSD95.

Results

Acetylation affects the localization of postsynaptic proteins

Several studies showed that acetylation plays important roles in LTP, and that enhancing acetylation by inhibiting HDACs facilitates LTP in the hippocampus and amygdala (Sharma, 2010). To assess the effect of protein acetylation on synapse composition we performed quantitative immunofluorescence analysis of the expression of the postsynaptic scaffold protein of excitatory synapses PSD95 (Fig. 1A), and of the presynaptic vesicular glutamate transporter VGLUT1 (Fig. 1B), in hippocampal neurons at 15 DIV, treated for 12 h with trichostatin A (TSA), an inhibitor of types I and II histone deacetylases. Neurons treated with TSA showed a significant increase in the fluorescence intensity, area and density of PSD95

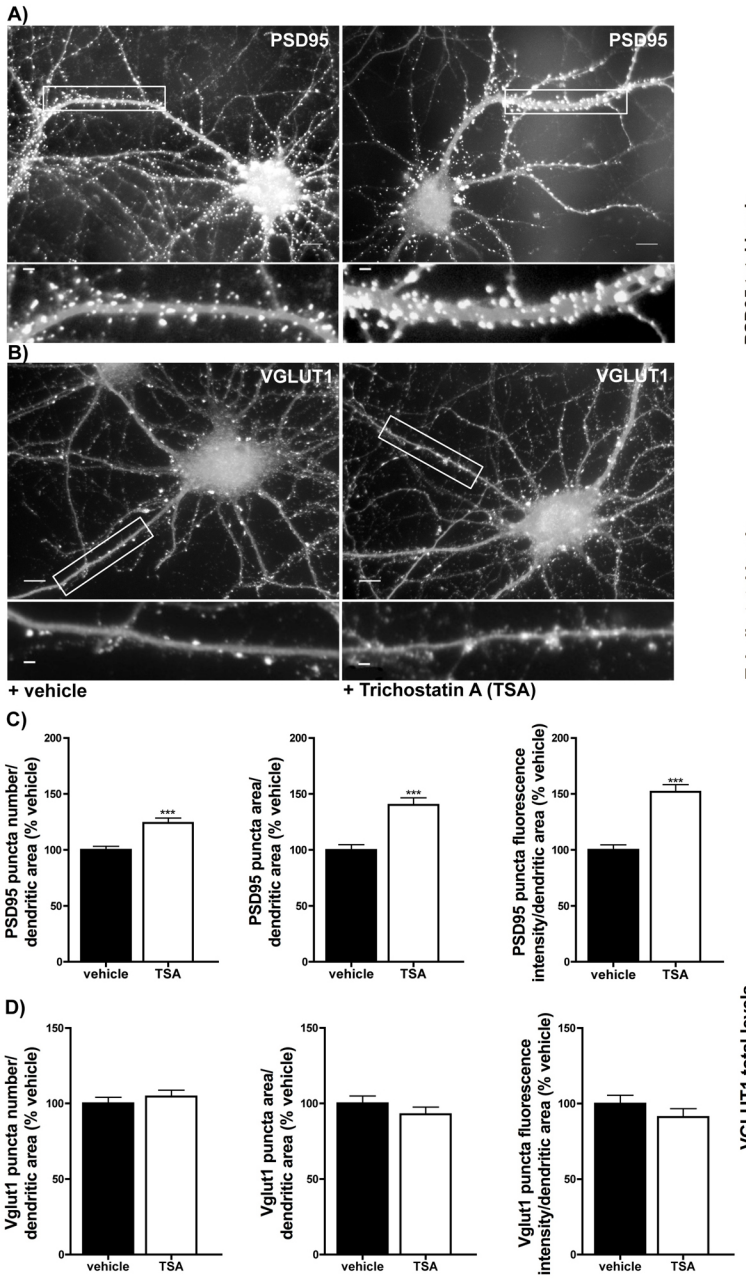

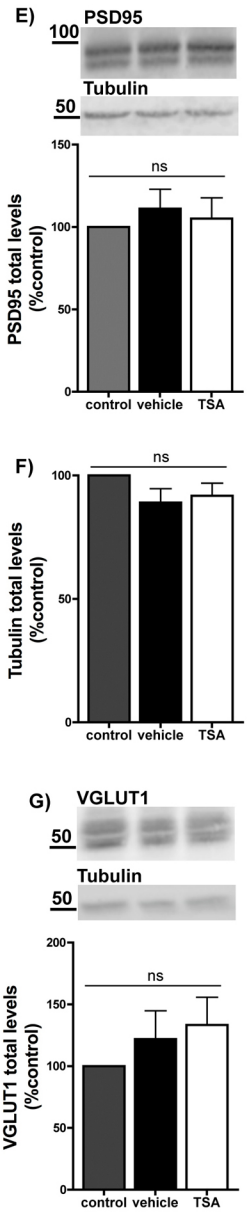

Fig. 1. Incubation of cultured hippocampal neurons with the HDACI/II inhibitor trichostatin A (TSA) leads to an increase in PSD95 clustering. Hippocampal neurons at 15 DIV were treated with vehicle or TSA (400 ng/ml) for 12 h. Neurons were stained for PSD95 (**A**) or VGLUT1 (**B**) and for the somatodendritic marker MAP2. Scale bars: 10 μm; enlarged images, 2 μm. Neurons were analyzed for PSD95 (**C**) and VGLUT1 (**D**) cluster fluorescence intensity, area and number, per dendritic area. Results are presented as percentage of vehicle-treated control cells, and are averaged from three (VGLUT1) and four (PSD95) independent experiments ($n \geq 64$ cells). Error bars show ±s.e.m. Significance, $^{***}P<0.001$ relative to control neurons (unpaired Student's *t*-test). (**E**–**G**) TSA treatment does not change PSD95, VGLUT1 or tubulin expression levels. Hippocampal neurons at 15 DIV were treated with vehicle or TSA (400 ng/ml) for 12 h. Western blot was performed using an anti-PSD95 (E), an anti-VGLUT1 (G) or an anti-tubulin (F) antibody. Data are presented as mean±s.e.m. of five experiments (for PSD95), nine experiments (tubulin) or three experiments (VGLUT1) performed in independent preparations, and are expressed as a percentage of protein expression levels in control conditions. Data were statistically analyzed using one-way ANOVA.

clusters (Fig. 1C), whereas no differences were observed for VGLUT1 clusters (Fig. 1D). The effect of TSA on the clustering of PSD95 could be due to an effect on the protein expression levels. Therefore, we assessed total protein levels by western blot (Fig. 1E–G), and found no detectable changes in total PSD95 (Fig. 1E), tubulin (Fig. 1F) or VGLUT1 (Fig. 1G) protein levels. These observations suggest that protein acetylation is correlated with the accumulation of PSD95 at synapses, and this accumulation may be due to redistribution of the protein.

To further investigate the effect of TSA on excitatory synapses, we analyzed Shank1 (Fig. 2A), another scaffold protein of excitatory synapses. TSA-treated neurons showed a significant increase in the fluorescence intensity of total dendritic Shank1 clusters, as well as in the density and area of those clusters (Fig. 2C). The Shank1 clusters that colocalized with VGLUT1 (synaptic clusters) were also increased in TSA treated neurons (Fig. 2D), whereas no changes on total Shank1 protein levels were detected (Fig. 2F). These observations suggest that protein acetylation, promoted by inhibition of HDACs, is correlated with the accumulation of Shank1 at synapses, due to redistribution of Shank1. To understand if the TSA effect is specific for excitatory synapses, we tested whether this treatment could affect proteins specific to inhibitory synapses (Fig. 2B). TSA had no effect on total dendritic gephyrin clusters (data not

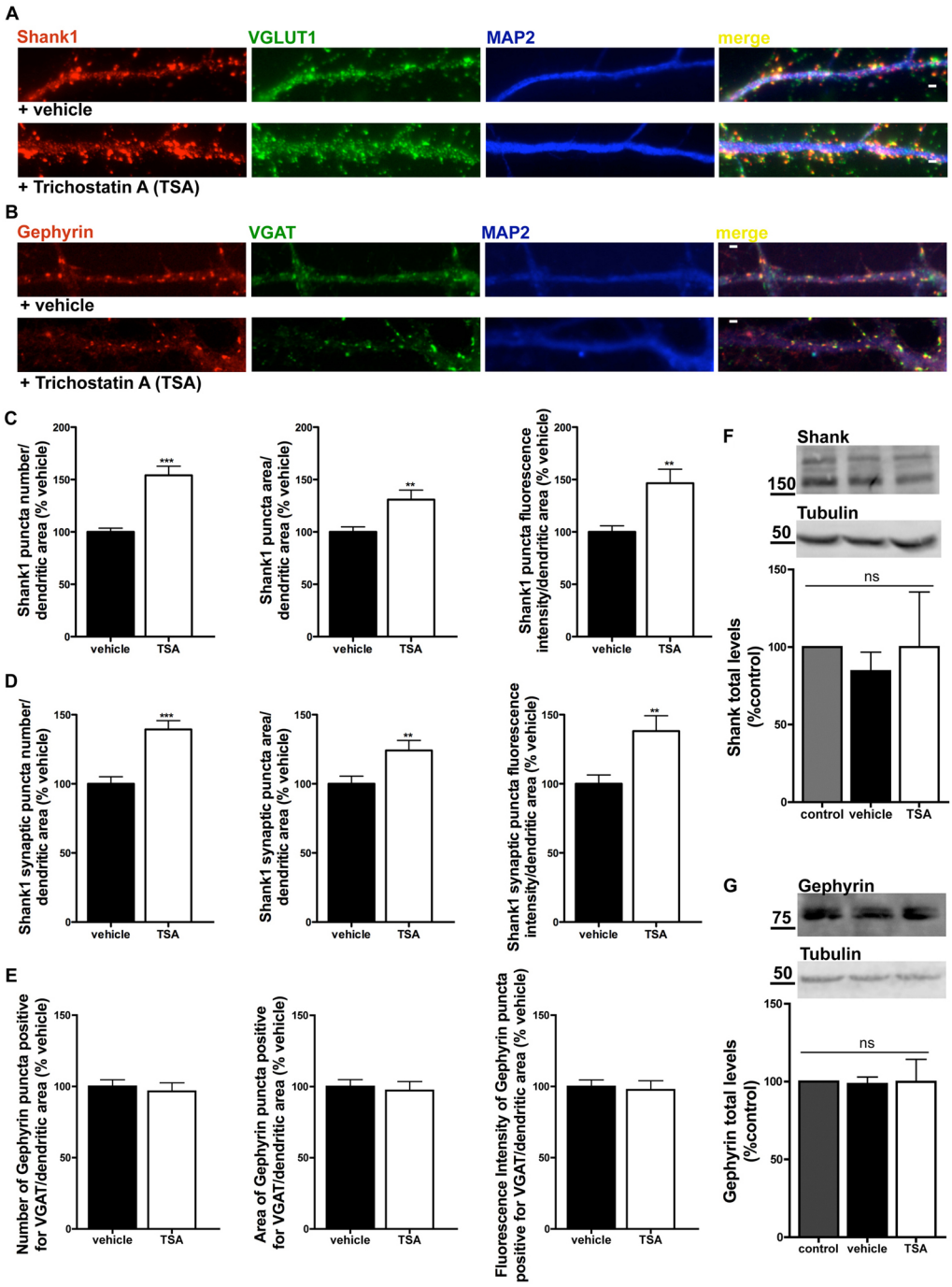

Fig. 2. Incubation of hippocampal neurons with TSA leads to an increase in synaptic Shank1 but does not affect gephyrin clustering. Hippocampal neurons at 15 DIV were treated with vehicle or TSA (400 ng/ml) for 12 h. Neurons were stained for MAP2 and (**A**) for Shank1, VGLUT1 or (**B**) for gephyrin and VGAT. Scale bars: 2 µm. Neurons were analyzed for total (**C**) and synaptic (**D**) Shank1 cluster fluorescence intensity, area and number, per dendritic area. Synaptic Shank1 is defined as Shank1 signal that overlaps with VGLUT1. Neurons were analyzed for total (data not shown) and synaptic (**E**) gephyrin clusters fluorescence intensity, area and number, per dendritic length. Synaptic gephyrin is defined as gephyrin signal that overlaps with VGAT. Results are presented as percentage of vehicle-treated cells, and are averaged from three independent experiments ($n \geq 60$ cells). Error bars show ±s.e.m. Significance: $^{**}P<0.01$, $^{***}P<0.001$ relative to control neurons (unpaired Student's *t*-test). (**F**,**G**) TSA treatment does not change Shank or gephyrin total expression levels. Hippocampal neurons were treated with vehicle or TSA for 12 h. Western blot was performed using an anti-panShank (F) or an anti-gephyrin antibody (G). Staining for tubulin was used for normalization of Shank and gephyrin expression level. Data are presented as mean±s.e.m. of three experiments performed in independent preparations, and are expressed as a percentage of Shank or gephyrin expression levels in control conditions. Data were statistically analyzed using one-way ANOVA. $P>0.05$.

shown), or on gephyrin clusters colocalized with the presynaptic vesicular GABA transporter (VGAT) (Fig. 2E), or on total gephyrin protein levels (Fig. 2G). Since the inhibition of HDACs with TSA had a significant effect on the clustering of postsynaptic scaffold proteins such as PSD95 and Shank1, we investigated whether this treatment could interfere with the clustering of AMPA receptors at the membrane. Quantitative immunofluorescence analysis was performed for the expression of synaptic cell surface GluA1-containing AMPA receptors in hippocampal neurons at 15 DIV (supplementary material Fig. S1). TSA treatment had no effect on total or synaptic GluA1 clusters (supplementary material Fig. S1A,C,D).

We then sought to determine if protein acetylation affects actin cytoskeleton proteins, since actin is a major component of dendritic spines. We focused on cortactin and p140Cap. Cortactin is an activator of the Arp2/3 actin nucleation machinery which is enriched in dendritic spines, where it co-localizes and interacts with F-actin and with the PSD scaffold Shank. Cortactin can regulate spine morphology, and mediates the interaction between actin and microtubules. In fact, recent work showed that dynamic microtubules can enter dendritic spines and affect actin dynamics (Jaworski et al., 2009). p140Cap is a binding partner for the microtubule plus-end tracking protein EB3, as well as for cortactin (Jaworski et al., 2009). We found that in hippocampal neurons treated with TSA the area and the fluorescence intensity of VGLUT1-colocalized p140Cap clusters is significantly decreased (Fig. 3A,C), whereas total p140Cap protein levels were unchanged (Fig. 3E). Additionally, the area of both total and VGLUT1-colocalized cortactin clusters decreased (Fig. 3D), but no alterations in total cortactin expression levels were detected (Fig. 3F). TSA treatment had no effect in the number or size of synaptic or total F-actin clusters (supplementary material Fig. S1F,G). Taken together, these observations suggest that protein acetylation correlates with a decrease in the area of

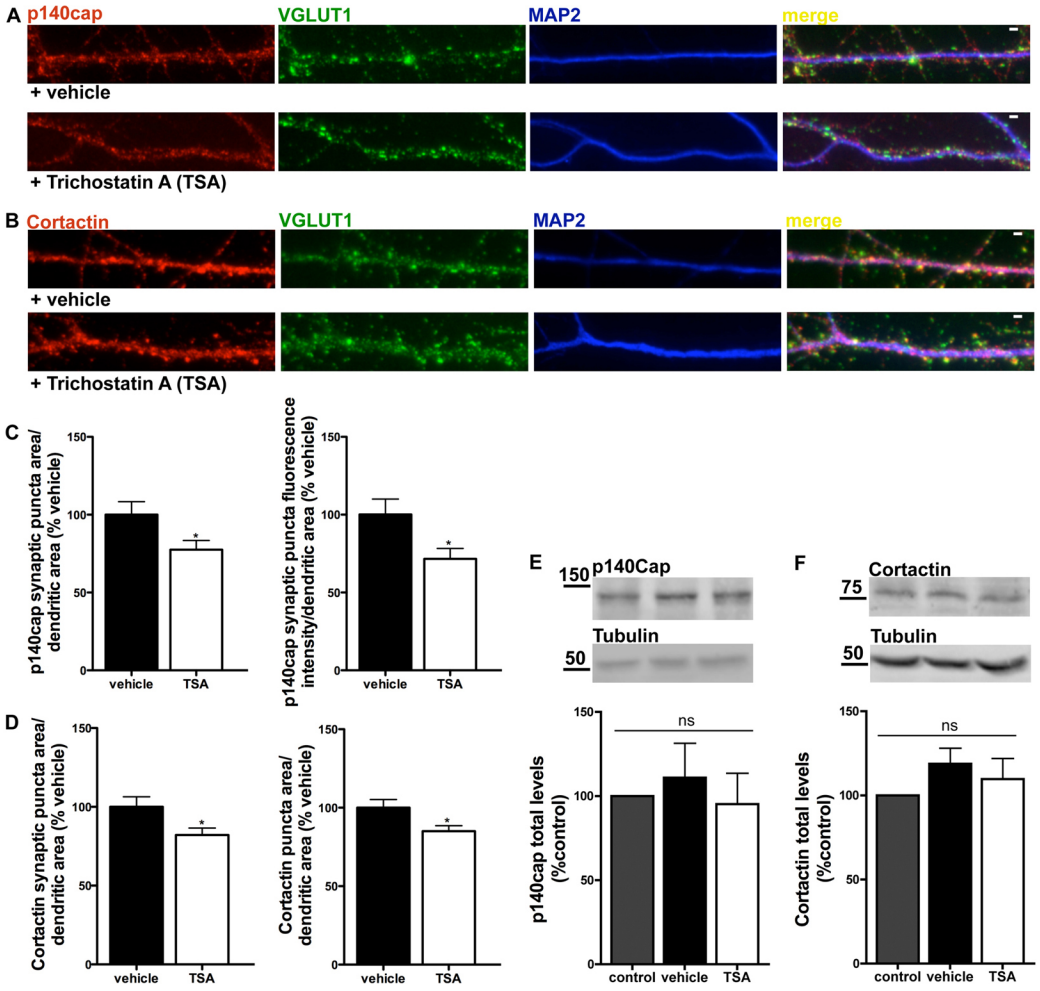

Fig. 3. TSA treatment of hippocampal neurons leads to a decrease in the area of synaptic p140Cap and cortactin clusters. Hippocampal neurons were treated with vehicle or TSA for 12 h. Neurons were stained for p140Cap (**A**) or cortactin (**B**), VGLUT1 and MAP2. Scale bars: 2 μm. Neurons were analyzed for total (data not shown) and synaptic p140Cap (**C**) or cortactin (**D**) cluster fluorescence intensity, area and number, per dendritic area. Synaptic p140Cap or cortactin signal is defined as overlapping with VGLUT1. Results are presented as percentage of vehicle control cells, and are averaged from three (for p140Cap) or four (for cortactin) independent experiments ($n \geq 63$ cells). Error bars show ±s.e.m. *$P<0.05$ relative to control neurons (unpaired Student's *t*-test). (**E**,**F**) TSA treatment does not change p140Cap or cortactin expression levels. Hippocampal neurons were treated with vehicle or TSA for 12 h. Western blot was performed using an anti-p140Cap (E) or an anti-cortactin (F) antibody. Staining for tubulin was used for normalization of p140Cap and cortactin values. Data are presented as mean±s.e.m. of three experiments performed in independent preparations, and are expressed as a percentage of p140Cap or cortactin expression levels in control conditions. Data were statistically analyzed using one-way ANOVA. $P>0.05$.

clusters of two cytoskeleton-related proteins at synapses, probably due to their redistribution from dendritic spines to shafts.

Cortactin acetylation affects its synaptic localization

Since cortactin is a substrate for acetylation in cancer cells (Zhang et al., 2007), we tested whether neuronal cortactin is regulated by acetylation. The levels of acetylated cortactin were assessed by western blot analysis using an antibody against acetylated cortactin (Zhang et al., 2007). Neuronal cortactin is acetylated in control conditions, and TSA treatment (12 h) led to an increase on the acetylation level of cortactin (Fig. 4A). Cortactin concentrates in dendritic spines of hippocampal neurons (Hering and Sheng, 2003). To characterize the

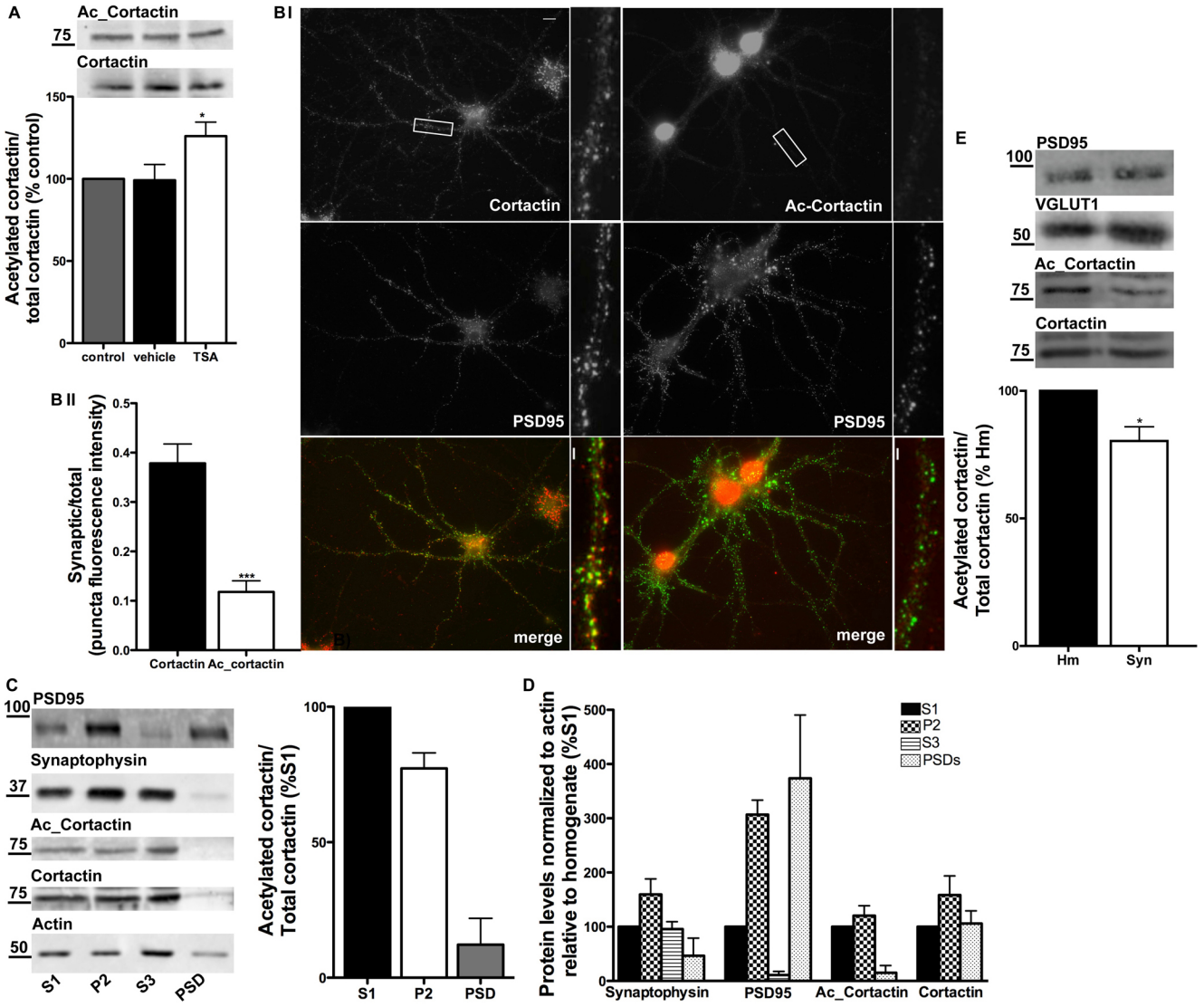

Fig. 4. Cortactin acetylation in hippocampal neurons. (**A**) Hippocampal neurons were treated with vehicle or TSA for 12 h. Western blot was performed using anti-acetylated cortactin (Ac_Cortactin) and anti-cortactin antibodies. Data are presented as mean±s.e.m. of 13 experiments performed in independent preparations, and are expressed as a percentage of cortactin acetylation in control conditions. Data were statistically analyzed using one-way ANOVA (*P<0.05, Dunnett's Multiple Comparison Test). (**BI**) Acetylated cortactin is less abundant in synapses. Hippocampal neurons at 15 DIV were stained with an antibody for cortactin, or an antibody for acetylated cortactin. Synaptic localization was determined by colocalization with the excitatory postsynaptic marker PSD95. Scale bars: 10 µm; enlarged images, 2 µm. (**BII**) The graph shows the fraction of total dendritic cortactin or acetylated cortactin puncta that colocalized with PSD95. Data were statistically analyzed using Student's t-test, n=16 cells, ***P<0.0001. (**C**) Synaptic profile of non-nuclear fraction (S1), crude synaptosomes (P2), crude synaptical vesicle fraction (S3) and postsynaptic densities (PSD) isolated from rat hippocampus. Western blot was performed using the following antibodies: anti-PSD95, anti-synaptophysin, anti-acetylated cortactin, anti-cortactin and anti-actin. Quantitative analysis was performed with ImageQuant. Data represent two experiments, and are expressed as a percentage of cortactin acetylation in the S1 fraction. Equal amounts of protein were applied to each lane. (**D**) The plot represents protein enrichment in each fraction, normalized to actin levels, and is expressed as a percentage of the S1 fraction. (**E**) Western blot profiles of total homogenate (Hm) and synaptoneurosome fractions (Syn) from rat hippocampus were performed using anti-PSD95, anti-VGLUT1, anti-acetylated cortactin and anti-cortactin antibodies. Data are presented as mean±s.e.m. of five experiments performed in independent preparations, and are expressed as a percentage of cortactin acetylation in total homogenate condition. Data were statistically analyzed using paired Student's t-test; *P<0.05.

neuronal localization of acetylated cortactin, hippocampal neurons at 15 DIV were double-stained with antibodies for the postsynaptic marker PSD95 and for cortactin or for the acetylated form of cortactin (Fig. 4B). Cortactin was found to strongly localize to synapses, with 37.85±0.04% of total dendritic cortactin co-localizing with PSD95, which is in accordance with previous studies showing a synaptic enrichment of the protein (Hering and Sheng, 2003; Racz and Weinberg, 2004). However, acetylated cortactin immunoreactivity was only residually present at synapses (11.79±0.02% of the dendritic protein co-localized with PSD95), and concentrated in neuronal cell bodies and dendritic shafts (Fig. 4B). To further evaluate the subcellular localization of acetylated cortactin, we biochemically isolated postsynaptic densities (PSDs) from hippocampi of adult rats. Western blot analysis showed that synaptophysin is enriched in synaptosomes and in the crude synaptic vesicle fraction, but not in the PSDs, whereas PSD95 is enriched in PSDs and absent from the crude synaptic vesicles fraction (Fig. 4C,D), indicating that the subsynaptic fractions obtained display the expected differential expression of post- and presynaptic proteins. When compared with total cortactin, acetylated cortactin is less enriched in the synaptic fractions, since we observed smaller amounts in the crude synaptosomes and only vestigial amounts in the isolated PSDs (Fig. 4C). The ratio of acetylated to total cortactin (Fig. 4C) or of acetylated cortactin to actin (Fig. 4D) were in fact reduced in the PSDs compared to other fractions. Additionally, to confirm the subcellular localization of acetylated cortactin, we used a preparation of synaptoneurosomes, which contains the presynaptic (synaptosome) and postsynaptic (neurosome) vesicularized components. We found that acetylated cortactin to total cortactin ratio is lower in synaptoneurosomes than in total hippocampal homogenates (Fig. 4E), whereas the synaptic markers PSD95 and VGLUT1 were enriched in these structures (Fig. 4E). Taken together, these data suggest that acetylation of cortactin triggers its redistribution from spines to dendritic shafts.

Acetylation of cortactin: role in PSD95 clustering

It has been shown that cortactin plays a role in the morphogenesis of spines (Hering and Sheng, 2003). Knockdown of cortactin by short-interfering RNA (siRNA) results in depletion of dendritic spines in hippocampal neurons, whereas overexpression of cortactin causes elongation of spines. Correlating with loss of spines, the density of PSD95 clusters on dendrites of cortactin-deficient neurons was diminished (Hering and Sheng, 2003). Having observed that neuronal cortactin is a substrate for acetylation (Fig. 4), and that protein acetylation promotes PSD95 clustering (Fig. 1), we tested whether acetylation of cortactin can influence the clustering of PSD95. To perform these experiments, we resorted to specific acetylation mimetic forms of cortactin. Nine out of the eleven lysine residues which have been identified as targets for acetylation (Zhang et al., 2007) are within the repeat region of cortactin. In order to mimic the non-acetylated form of cortactin we used a charge preserving cortactin mutant in which all of the nine repeat-region lysines were mutated to arginine (9KR), and which is able to efficiently bind F-actin (Zhang et al., 2007). To mimic the acetylated form of cortactin we used a charge-neutralizing cortactin mutant in which all nine of the repeat-region lysine residues were mutated to glutamine (9KQ) and which is not able to bind F-actin. Hippocampal neurons were transfected with GFP together with wild-type FLAG-tagged cortactin, or the FLAG-tagged mimetic mutants for acetylated or deacetylated cortactin. Neurons were triple-stained with antibodies against PSD95, the FLAG epitope and MAP2 (Fig. 5A). Transfected neurons were identified by GFP fluorescence, and the FLAG signal was observed for confirmation of overexpression of the cortactin constructs. Quantitative analysis of the PSD95 signal showed that in neurons transfected with the mutant that mimics the deacetylated form of cortactin (9KR) the fluorescence intensity and area of PSD95 clusters are decreased (Fig. 5B), whereas no changes relatively to control cells were observed in neurons expressing wild-type cortactin or the mutant form of cortactin that mimics the acetylated protein (9KQ). These data suggest that acetylation of cortactin may be required for the clustering of PSD95 in synapses.

Since we overexpressed wild-type cortactin or the acetylation mutants for cortactin in hippocampal neurons expressing endogenous cortactin, interpretation of the observed effects is confounded by the functional role of the endogenous protein, which is likely a combination of acetylated and non-acetylated cortactin. To further assess the effect of cortactin acetylation on excitatory synapses we used a previously described short-hairpin RNA (shRNA) sequence against cortactin to knockdown the expression of endogenous cortactin (Hering and Sheng, 2003). We used the pLentiLox3.7(CMV)EGFP vector, which was engineered by introducing the mouse U6 promoter upstream of a cytomegalovirus promoter-based GFP expression cassette to create a vector that simultaneously produces cortactin shRNA and GFP, allowing us to easily identify shRNA-transfected neurons. Hippocampal neurons in culture were transfected at 12 DIV with cortactin-shRNA and analyzed at 15 DIV for cortactin expression (supplementary material Fig. S2). The cortactin-shRNA construct decreased the dendritic fluorescence intensity of cortactin clusters to 51.7±5.8% of neurons transfected with control shRNA. The clustering of PSD95 was evaluated in neurons expressing control shRNA and in neurons expressing cortactin-shRNA (Fig. 6A). The knockdown of cortactin in hippocampal neurons at this age results in a decrease in the density and intensity of PSD95 clusters (Fig. 6B). In order to exclude the contribution of off-target effects of the cortactin-shRNA, a rescue construct was generated with silent mutations in the cortactin region targeted by the cortactin-shRNA. In neurons co-transfected with the cortactin-shRNA plasmid and the cortactin construct refractory to cortactin-shRNA-mediated knockdown (Cortactin-wt*), the density and fluorescence intensity of PSD95 clusters were rescued to levels similar to those observed in neurons transfected with the control shRNA (Fig. 6B). These results indicate that the defects observed for PSD95 clustering with cortactin-shRNA are specifically due to the loss of cortactin. Furthermore, we tested the ability of acetylation mutants of cortactin insensitive to the cortactin-shRNA to rescue the decrease on PSD95 clustering observed upon loss of endogenous cortactin. Expression in hippocampal neurons of the acetylated cortactin mimetic mutant (Cortactin-9KQ*) rescued the cortactin-shRNA-mediated decrease on the density and intensity of PSD95 clusters (Fig. 6B). On the other hand, expression of the deacetylated mimetic form of cortactin (Cortactin-9KR*) could not rescue the cortactin-shRNA-mediated decrease on PSD95 clustering. These observations indicate that the acetylation of cortactin is important for its effect on PSD95 clustering.

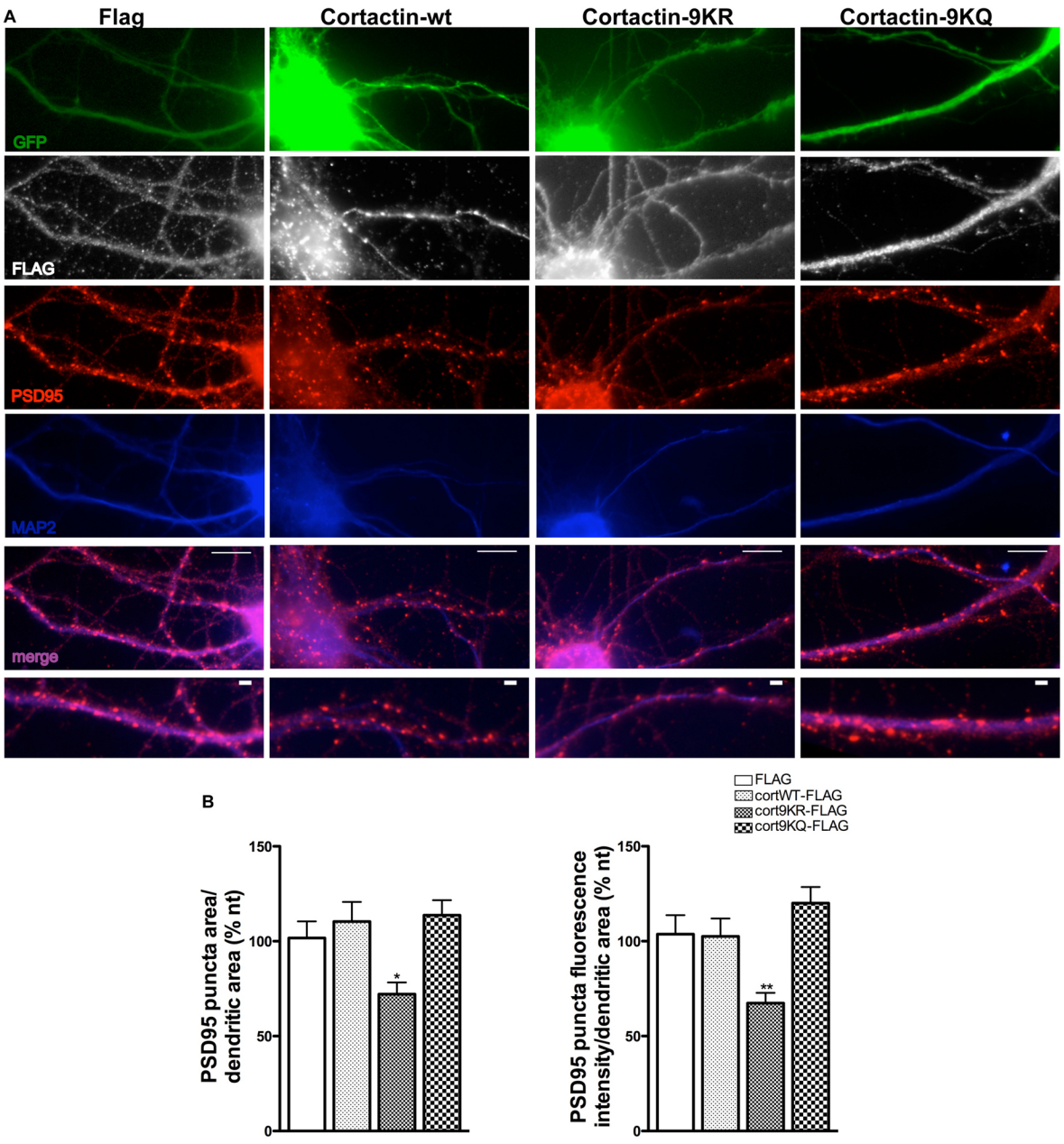

Fig. 5. Acetylation of cortactin may be required for PSD95 clustering. (**A**) Hippocampal neurons were transfected at 7 DIV with GFP along with the empty vector (FLAG), cortactinWT-FLAG, cortactin9KR-FLAG or cortactin9KQ-FLAG. Neurons (15 DIV) were stained for FLAG, MAP2 and PSD95. Transfected neurons, identified by GFP fluorescence, were analyzed for PSD95 cluster fluorescence intensity, number and area, per dendritic area. Scale bars: 10 µm; enlarged images, 2 µm. (**B**) Results are presented as percentage of control cells (transfected with empty vector), and are averaged from four independent experiments ($n \geq 28$ cells). Error bars show s.e.m. Significance: $^{*}P<0.05$, $^{**}P<0.01$, relative to non-transfected neurons (one-way ANOVA followed by Dunnett's Multiple Comparison Test).

We then tested whether neuronal treatment with TSA still affects PSD95 clustering in neurons where cortactin expression was downregulated with cortactin-shRNA. Hippocampal neurons were transfected with control shRNA or cortactin-shRNA and the clustering of PSD95 was analyzed in control conditions and in neurons treated with TSA. Similarly to what was observed for non-transfected neurons (Fig. 1A,C), neurons transfected with control shRNA showed an increase on the fluorescence intensity of PSD95 clusters to 132.2% of control neurons (Fig. 6C). Interestingly, in neurons transfected with cortactin-shRNA TSA could still produce a 26.9% increase on the intensity of PSD95 clusters, even though the fluorescence intensity of PSD95 clusters was still below control levels, even after TSA treatment. This evidence suggests that, either the remaining endogenous cortactin, after knockdown with cortactin-shRNA, is sufficient for the treatment with TSA to cause an effect on PSD95, or that besides causing an increase on cortactin acetylation and thereby influencing PSD95 clustering, the TSA treatment promotes the acetylation of other protein targets which affect PSD95 clustering. In agreement with this idea, the effect of

TSA on PSD95 clustering was also observed in neurons in which the endogenous cortactin was knocked down and the acetylation-resistant (9KR) mutant of cortactin was re-introduced (Fig. 6C). Importantly, when the acetylation mimetic mutant of cortactin (9KQ) was introduced in neurons transfected with cortactin shRNA not only were the basal levels of PSD95 clustering recovered but we could no longer detect an effect for TSA on PSD95 clustering (Fig. 6C). Altogether these results support the idea that cortactin acetylation promotes PSD95 clustering; acetylation of other protein targets may contribute to the same effect through mechanisms that are redundant with those triggered by cortactin acetylation.

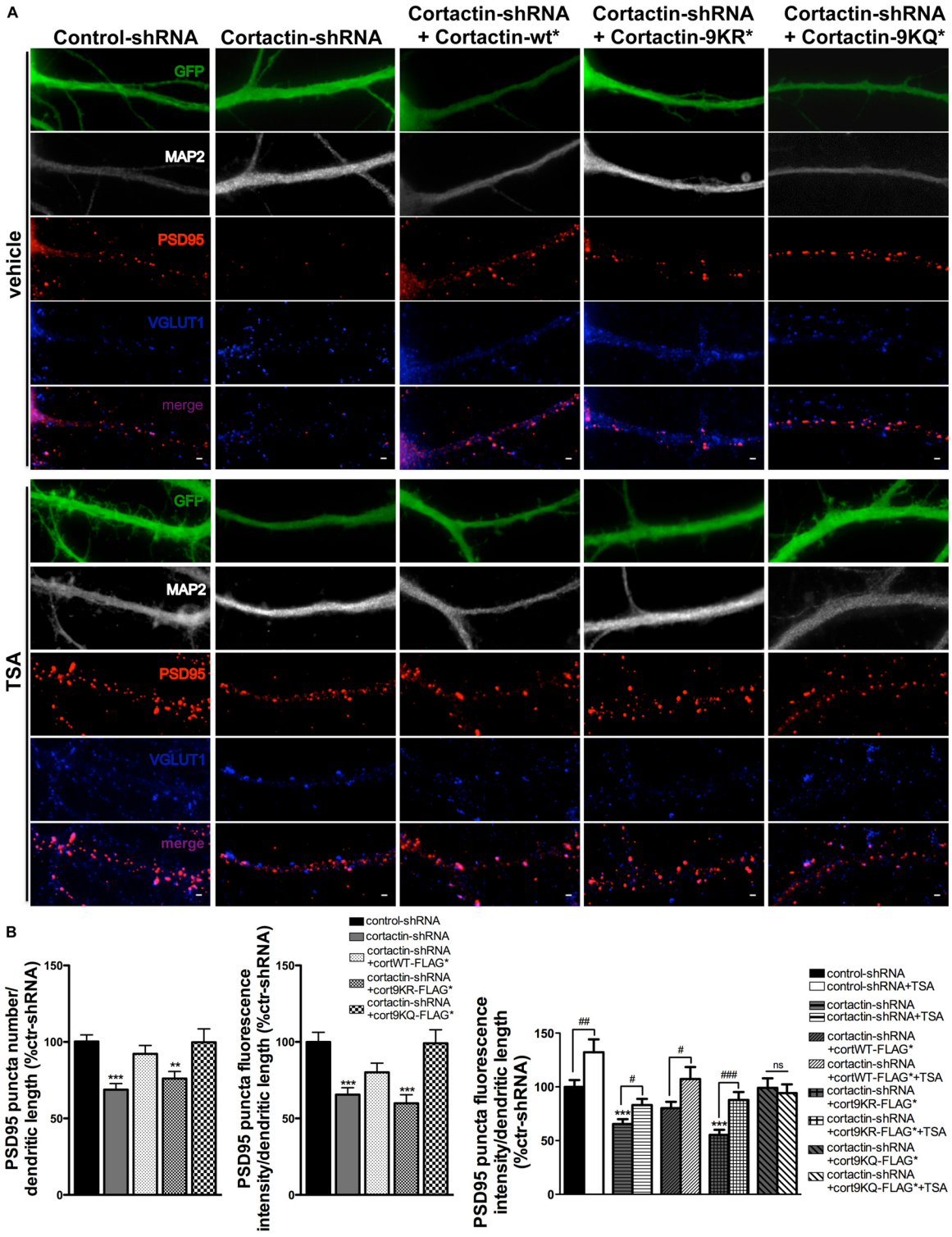

Fig. 6. See next page for legend.

Since our data suggest that other targets for protein acetylation besides cortactin are likely to influence PSD95 clustering in dendrites, we tested whether Shank, PSD95 or p140Cap are acetylated. We immunoprecipitated these proteins from cultured hippocampal neurons and used an anti-acetyl-lysine antibody to test for their acetylation or for the acetylation of interacting proteins present in the immunoprecipitated sample. We found no conclusive evidence for the acetylation of Shank1 (supplementary material Fig. S3A) or PSD95 itself, but repeatedly identified three acetylated high-molecular weight bands corresponding to proteins that co-precipitate with PSD95 (supplementary material Fig. S3B). Interestingly, p140Cap immunoprecipitated from hippocampal neurons was labeled for acetylation, but its acetylation did not overtly change with the TSA treatment (supplementary material Fig. S3C). These are intriguing observations that deserve to be further explored and may lead to the identification of other molecular targets for acetylation that influence synapse composition and function.

It was previously reported that dendrites of cortactin-deficient neurons not only show a decrease in the density of protrusions and of PSD95 clusters, but also in the density of F-actin clusters (Hering and Sheng, 2003). Therefore, we sought to investigate if acetylation of cortactin promotes changes in the density and size of F-actin clusters. Surprisingly, in our experimental conditions knockdown of cortactin at 12 DIV did not change the number or size of dendritic F-actin clusters at 15 DIV (supplementary material Fig. S4). Additionally, reintroduction of wild-type cortactin or the acetylation mimetic mutants of cortactin did not significantly change F-actin clustering in dendrites (supplementary material Fig. S4). These evidence do not exclude effects of cortactin acetylation on the morphology or dynamics of spines, but indicate that the effects observed for PSD95 clustering (Figs. 5,6) are likely not secondary to changes in F-actin clustering.

Fig. 6. Knockdown of cortactin decreases PSD95 clustering, an effect rescued by acetylated cortactin. (**A**) Hippocampal neurons were transfected at 12 DIV with control shRNA, with the cortactin-shRNA construct or co-transfected with the cortactin-shRNA construct along with constructs encoding shRNA resistant cortactinWT-FLAG*, cortactin9KR-FLAG* or cortactin9KQ-FLAG*. Control neurons or TSA-stimulated neurons were stained for MAP2 and PSD95 and VGLUT. Transfected neurons at 15 DIV, identified by GFP fluorescence, were analyzed for PSD95 cluster number and fluorescence intensity. Scale bar: 2 μm. (**B**) The effect of cortactin-shRNA on PSD95 clustering can be rescued by wild-type cortactin and by the acetylated cortactin mimetic mutant. Results are presented as percentage of control shRNA-expressing cells, and are averaged from five independent experiments ($n \geq 30$ cells). Error bars show ±s.e.m. Significance: $^{**}P<0.01$, $^{***}P<0.001$, relative to control shRNA-transfected neurons (one-way ANOVA followed by Dunnett's Multiple Comparison Test). (**C**) The effect of TSA on the fluorescence intensity of PSD95 clusters can be detected in cells in which endogenous cortactin was knocked down, and in cells in which wild-type or the deacetylated mimetic mutant of cortactin have been reintroduced, but not when the acetylated cortactin mimetic mutant is re-expressed. Results are presented as percentage of control shRNA-expressing cells, and are averaged from three to six independent experiments ($n \geq 24$ cells). Error bars show ±s.e.m. Significance: $^{**}P<0.01$, $^{***}P<0.001$, relative to control shRNA-transfected neurons (one-way ANOVA followed by Dunnett's Multiple Comparison Test); $^{\#}P<0.05$, $^{\#\#}P<0.01$, $^{\#\#\#}P<0.001$, relative to control (without TSA) for each transfection condition (*t*-test).

Cortactin acetylation regulates its tyrosine phosphorylation and protein–protein interactions

The phosphorylation of cortactin and the resulting functional consequences have been an intense area of study. Phosphorylation of cortactin by Src has consequences with regards to actin dynamics, possibly affecting the ability of cortactin to bind to and cross-link actin filaments (Ammer and Weed, 2008). In order to test if the acetylation status of cortactin regulates its Y421 phosphorylation, HEK 293 FT cells were transfected with the FLAG-tagged wild-type and acetylation mimetic forms of cortactin, and the levels of cortactin phosphorylated at Y421 were assessed by western blot. Notably, the Y421 phosphorylation levels of the deacetylated cortactin mimetic mutant are higher than those of the acetylated cortactin mimetic mutant (Fig. 7A). We then tested whether cortactin acetylation affects its interaction with Src. FLAG-tagged wild type or acetylation mimetic forms of cortactin were immunoprecipitated, and the co-precipitation of endogenous Src was evaluated. Src preferentially co-immunoprecipitated with the deacetylated cortactin mimetic mutant (Fig. 7B, 4.2±0.7-fold higher interaction of Src with the deacetylation-mimetic than with the acetylation-mimetic mutant), in agreement with the higher levels of tyrosine phosphorylation of this mutant (Fig. 7A). Given the evidence that cortactin phosphorylation can regulate its interactions with SH3 binding proteins, and our observation that cortactin acetylation regulates its phosphorylation state (Fig. 7A), we tested whether acetylation of cortactin interferes with its binding to synaptic proteins. It has been shown that cortactin interacts through its SH3 domain with the Shank family of proteins that are localized to the PSD of excitatory synapses (Naisbitt et al., 1999), and through this interaction cortactin may stabilize postsynaptic clusters of glutamate receptors. Another known cortactin interactor is p140Cap. In order to study the interaction between cortactin in its acetylated and deacetylated forms and either Shank1 or p140Cap proteins, we performed co-immunoprecipitation experiments in an heterologous system. HEK 293 FT cells were co-transfected with the FLAG-tagged wild type or acetylation mimetic forms of cortactin, along with GFP-tagged Shank1 or GFP-tagged p140Cap. Immunoprecipitation of FLAG-tagged constructs resulted in the co-precipitation of both Shank1 and p140Cap (Fig. 7C). Notably, both p140Cap and Shank1 co-immunoprecipitated to higher levels with the deacetylated cortactin mimetic mutant than with the mutant that mimics acetylated cortactin (3.6±1.6-fold difference for p140Cap, 2.9±1.1-fold difference for Shank1). These results confirm that cortactin interacts with both Shank1 and p140Cap, and suggest that these interactions are modulated by the acetylation state of cortactin. In order to further test whether cortactin acetylation affects its interaction with Shank and p140Cap, we immunoprecipitated cortactin from cultured hippocampal neurons in control conditions or after incubation with TSA for 12 h. Both Shank and p140Cap co-immunoprecipitated with cortactin less efficiently in neurons treated with TSA than in control neurons (Fig. 7D), supporting the data obtained using transfected cells.

Effect of BDNF and glutamate on cortactin acetylation

There are no described stimuli in neurons, or in other cell types, that regulate acetylation of cortactin. The neurotrophin BDNF plays a key role in the regulation of the structure and function of

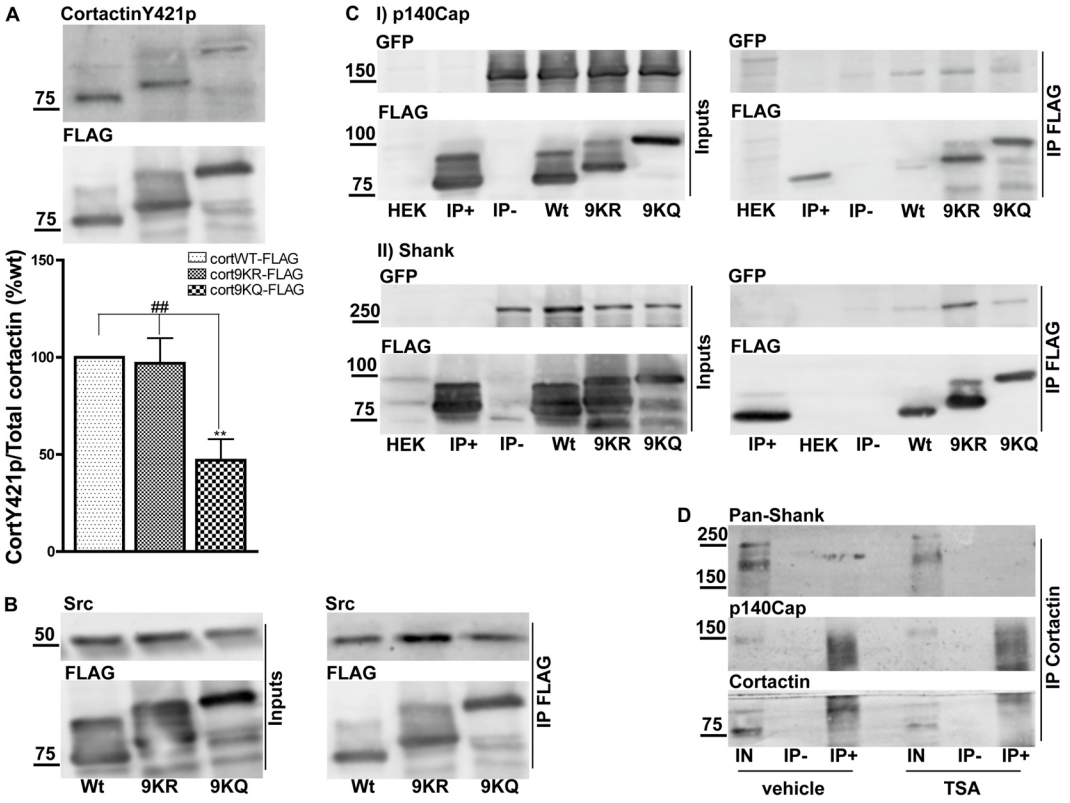

Fig. 7. Cortactin acetylation regulates its phosphorylation at tyrosine 421 and its association with Shank1 and p140Cap in HEK 293FT cells. (**A**) Wild-type FLAG-tagged cortactin or the FLAG-tagged cortactin acetylation mutant constructs were transfected in HEK 293FT cells. Cortactin phosphorylation levels were assessed by western blot using an antibody against phosphorylated cortactin at Y421, and normalized to total cortactin. Results are presented as percentage of wild-type cortactin, and are averaged from seven independent experiments. Error bars show s.e.m. Statistical significance was determined by one-way ANOVA. **Significant difference from the control with $P<0.01$ (Dunnett's post-hoc test) and ## indicates a significant difference from control and cort9KR-FLAG with $P<0.01$ (Bonferroni's post-hoc test). (**B**) Src preferentially interacts with the deacetylated form of cortactin. FLAG-tagged cortactin or its acetylation mutants were immunoprecipitated from transfected cells. Src co-immunoprecipitated preferentially with the deacetylated-cortactin mimetic mutant. Images are representative of two independent experiments. (**C**) Cortactin acetylation mutant constructs were co-transfected with p140Cap-GFP (I) or Shank-GFP (II) in HEK 293FT cells. Cortactin or its mutants were immunoprecipitated using an antibody against the FLAG epitope. Co-immunoprecipitation of either p140Cap or Shank was assessed with an antibody for GFP. HEK: non transfected cells; IP+: cells transfected with cortactin-FLAG only; IP-: cells transfected with p140Cap-GFP (I), or Shank1-GFP (II) only; Wt: cells co-transfected with GFP tagged proteins [either p140Cap (I) or Shank (II)] and cortactinWt-FLAG; 9KR: cells co-transfected with GFP tagged proteins and cortactin9KR-FLAG; 9KQ: cells co-transfected with GFP tagged proteins and cortactin9KQ-FLAG. The efficiency of immunoprecipitation was assessed by probing the immunoprecipitated samples for the FLAG epitope (lower panels), whereas the co-immunoprecipitation was assessed using an anti-GFP antibody (upper panels). Images are representative of three independent experiments. (**D**) The TSA treatment decreases the interaction between p140Cap and Shank with cortactin. Cortactin was immunoprecipitated from control or TSA (12 h) treated hippocampal neurons. The immunoprecipitated samples were immunoblotted for cortactin, p140Cap and Shank. IN, input.

the glutamatergic synapses (Carvalho et al., 2008). BDNF is secreted at synapses in response to activity (Pang et al., 2004), increases synaptic AMPA and NMDA receptors (Caldeira et al., 2007), induces the transport of PSD95 to dendrites (Yoshii and Constantine-Paton, 2007), and increases PSD95 in dendritic spines (Hu et al., 2011). BDNF has also been shown to promote cortactin redistribution in neurons (Iki et al., 2005). Therefore, we tested whether BDNF could change the acetylation state of cortactin in hippocampal neurons.

The acetylation of cortactin was assessed by western blot in control hippocampal neurons as well as in neurons treated with 100 ng/ml BDNF for 60 minutes. Neuron treatment with BDNF led to increased acetylation of cortactin in relatively mature hippocampal neurons (15 DIV, Fig. 8A), but not in developing neurons (7 DIV, Fig. 8B), and did not change the acetylation levels of tubulin (Fig. 8C), another cytoskeleton protein targeted for acetylation. Cortactin localization within neurons is not only regulated by BDNF, but also by NMDA receptor activity (Hering and Sheng, 2003; Iki et al., 2005; Seese et al., 2012). NMDA receptor activation induced cortactin redistribution from dendritic spines to the shaft (Iki et al., 2005), and LTP induction translocates cortactin from spines to synapses in an NMDA-receptor dependent manner (Seese et al., 2012). To test whether glutamate promotes acetylation of cortactin, hippocampal neurons were treated with 100 μM glutamate for 15 minutes. The levels of acetylated cortactin were increased (Fig. 8D), whereas the acetylation levels of tubulin were not altered (Fig. 8E) in response to glutamate treatment.

Discussion

We studied the effects of inhibiting types I and II HDACs with TSA on the localization of synaptic proteins, and found that TSA

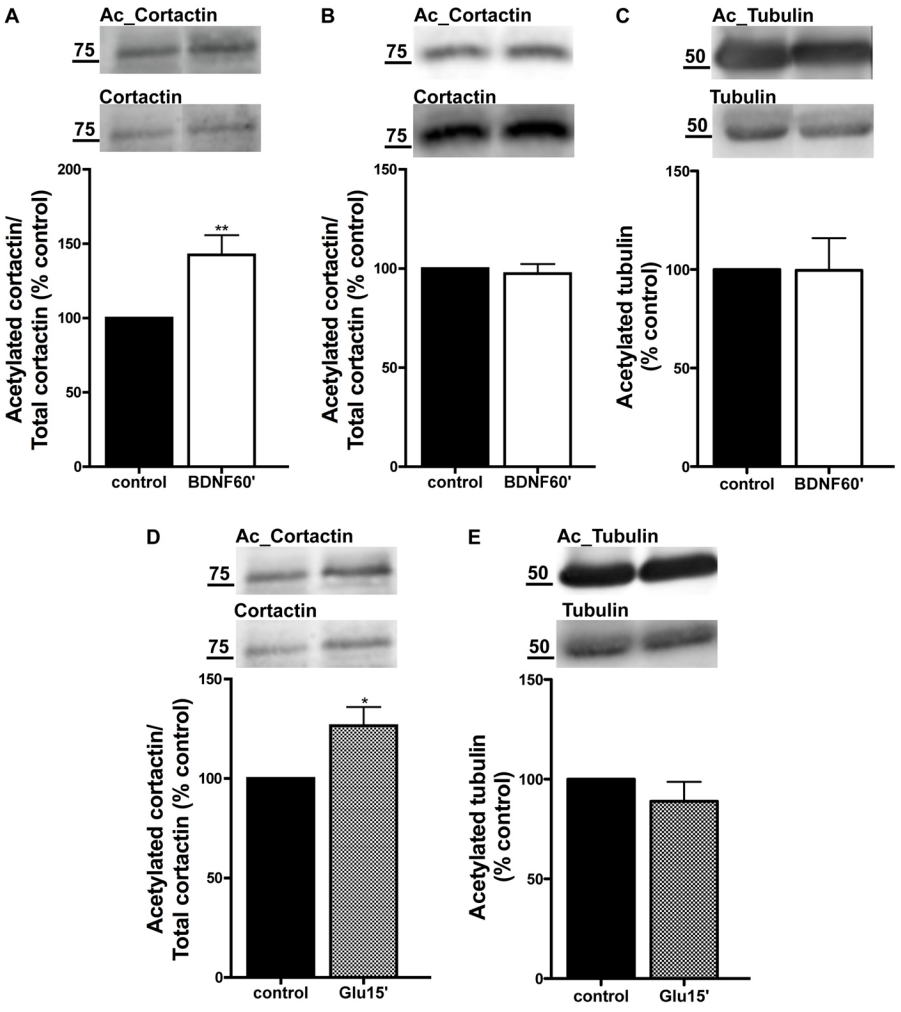

Fig. 8. Acetylation of cortactin is increased in response to BDNF and glutamate treatment. 15 DIV (**A**,**C**) and 7 DIV (**B**) hippocampal neurons were incubated with 100 ng/ml BDNF for 60 min. (**D**,**E**) Hippocampal neurons (15 DIV) were treated with glutamate (Glu, 100 μM) for 15 min. Western blot was performed using anti-acetylated tubulin (Ac_Tubulin), anti-acetylated cortactin (Ac-Cortactin), anti-tubulin and anti-cortactin antibodies. Data are presented as mean±s.e.m. of several experiments ($n \geq 5$) performed in independent preparations, and are expressed as a percentage of cortactin and tubulin acetylation in control conditions. Data were statistically analyzed using paired Student's *t*-test. $^{*}P<0.05$, $^{**}P<0.01$.

treatment of hippocampal neurons leads to an increase in PSD95 (Fig. 1A,C) and Shank1 (Fig. 2A,C,D) clusters. Conversely, HDACs inhibition resulted in decreased cluster area of the cytoskeleton associated proteins cortactin and p140Cap (Fig. 3), while VGLUT1 was unaffected (Fig. 1B,D). These data indicate that the composition of excitatory synapses is regulated by protein acetylation. The observed changes in synaptic composition do not seem to be direct effects of alterations in gene expression that could be mediated by histone acetylation. We studied the acetylation pattern of cortactin, and found that cortactin is a substrate for acetylation/deacetylation in neurons (Fig. 4A), and that cortactin acetylation has an impact on regulating PSD95 clustering. Overexpression of the deacetylated cortactin mimetic mutant in hippocampal neurons decreased the dendritic clustering of PSD95 (Fig. 5), and the mutant of cortactin that mimics the acetylated form of the protein rescued the defects in PSD95 clustering mediated by knockdown of cortactin with shRNA (Fig. 6A,B). Additionally, TSA produced an increase on PSD95 clustering in neurons in which cortactin was downregulated, indicating that the acetylation of other proteins besides cortactin can have an effect on PSD95 clustering; however, when the acetylated cortactin mimetic mutant of cortactin was reintroduced in neurons expressing cortactin-shRNA TSA no longer had an effect on PSD95 clustering, in agreement with the idea that cortactin acetylation is sufficient to mimic the TSA effect.

Our studies identify cortactin acetylation as a modification that can impact on its cellular localization in neurons. Immunocytochemical studies in cultured rat hippocampal neurons confirmed that cortactin is concentrated in dendritic spines, in agreement with previous studies (Hering and Sheng, 2003; Racz and Weinberg, 2004), whereas acetylated cortactin was found to be distributed throughout dendrites and cell bodies (Fig. 4B), and to be decreased in hippocampal synaptic fractions (Fig. 4C–E). In agreement with our data, it has been reported that acetylation of cortactin inhibits its Rac-mediated translocation to the cell periphery and its presence in membrane ruffles in transfected NIH 373 cells (Zhang et al., 2007). Our data showing that overexpression of the deacetylated cortactin mimetic mutant decreases the dendritic clustering of PSD95 (Fig. 5), whereas the mutant of cortactin that mimics its acetylated form rescues the defects in PSD95 clustering mediated by knockdown of cortactin (Fig. 6), suggest that cortactin acetylation and redistribution from the dendritic spine to the shaft may be removing an inhibitory effect of cortactin on the clustering of PSD95.

The effect of cortactin acetylation on PSD95 dendritic clustering may be independent from the function of cortactin as a regulator of actin dynamics, since the size and number of

F-actin clusters were not changed by knockdown of cortactin and reintroduction of the cortactin acetylation mutants that changed the fluorescence intensity and area of PSD95 clusters (supplementary material Fig. S4). A previous study showed that the synaptic clustering of PSD95 is unaffected by actin depolymerization, suggesting that PSD95 is a core scaffolding component and that its localization at synapses is independent of the actin cytoskeleton (Allison et al., 2000). This study suggests that F-actin is necessary for the initial formation or transport of the synaptic structure, but not for the maintenance of PSD95 at the postsynaptic density. Once a synapse has formed, actin dynamics is involved in mediating activity-dependent changes in spine morphology, rather than in the localization of core synaptic proteins. In agreement with this model, our data suggest that cortactin acetylation may affect PSD95 synaptic clustering independently of its effects on F-actin polymerization. However, our data do not exclude that cortactin acetylation may have an impact on the spine morphology, namely on the width or length of spines, or on spine motility.

We found that cortactin acetylation is increased by neuronal treatment with BDNF at 15 DIV, whereas no effect of BDNF was detected in younger neurons (Fig. 8A,B). BDNF has been previously found to trigger ERK-dependent cortactin translocation to dendritic spines in 12–16 DIV neurons (Iki et al., 2005), but this effect was not observed in more mature hippocampal neurons (20 DIV), indicating that BDNF may have different effects depending on the maturation stage of the culture (Iki et al., 2005). Moreover, LTP induction in hippocampal slices was recently shown to be associated with a decrease on synapse-associated cortactin which is accompanied by an increase on the phosphorylation of the serine residue targeted by ERK in cortactin (Seese et al., 2012), indicating that ERK phosphorylation is not single-handed in regulating the localization of synaptic cortactin, which is probably tightly regulated by a balance between different post-translational modifications. In our culture conditions, at 15 DIV BDNF promotes the acetylation of cortactin, which we find to lead to the relocalization of cortactin away from synapses.

Our findings are in accordance with the increase in PSD95 within spines after BDNF treatment in visual cortical neurons (Yoshii and Constantine-Paton, 2007). These authors showed that when BDNF is applied to cultured visual cortical neurons the size of PSD95 puncta in spines and the overall amount of PSD95 in dendrites are increased within 60 min. We saw that a 60-min BDNF treatment promotes cortactin acetylation in hippocampal neurons in culture (Fig. 8A), and we also observed that inhibition of HDACs activity leads to cortactin acetylation (Fig. 4A) and clustering of PSD95 in dendritic spines (Fig. 1A,C). It is therefore possible to speculate that cortactin acetylation plays a role in the BDNF-triggered accumulation of PSD95 in dendritic spines.

In addition, we found that cortactin acetylation is increased by neuronal treatment with glutamate at 15 DIV (Fig. 8D). NMDA receptor stimulation was described to induce cortactin redistribution from the spine to the shaft (Hering and Sheng, 2003) and this effect was attributed to Src-mediated phosphorylation of cortactin at tyrosine residues (Iki et al., 2005). We propose that glutamate-induced cortactin acetylation may also be involved in cortactin translocation from spines to the shafts of dendrites. Moreover, cortactin acetylation is negatively correlated with its tyrosine phosphorylation. The cortactin mutant that mimics deacetylation is more phosphorylated at Y421 than the acetylated cortactin mutant (Fig. 7A), and more efficiently binds to Src (Fig. 7B). These results are in agreement with a recent study showing that cortactin acetylation and its tyrosine phosphorylation are mutually exclusive (Meiler et al., 2012). These data also suggest that the acetylation-mediated redistribution of cortactin is not secondary to the tyrosine phosphorylation-mediated relocalization of cortactin to dendritic shafts. The role of tyrosine phosphorylation in the regulation of cortactin function, localization and interaction with other proteins is far from being fully understood, and contradictory evidence have been reported. Tyrosine phosphorylation of cortactin has been shown to increase cell motility and invasion *in vivo*, but has been reported to have both positive and negative effects on actin polymerization *in vitro* (Martinez-Quiles et al., 2004; Tehrani et al., 2007), and to promote cell migration by increasing the turnover of focal adhesions (Kruchten et al., 2008). Our data further support a role for cortactin acetylation in regulating its phosphorylation at tyrosine residues by Src.

Biochemical evidence demonstrated that the deacetylation mimetic mutant of cortactin not only interacts with Shank1 but also with the microtubule associated protein p140Cap, and that these interactions are reduced by cortactin acetylation (Fig. 7C,D). By transiently targeting dendritic spines, the function microtubules serve, along with the actin cytoskeleton, is likely to involve transport of essential proteins into and out of the spine (reviewed by Dent et al., 2011). Indeed the blockade of microtubule polymerization with nocodazole causes a decrease in the number of synapses associated with high concentrations of cortactin in hippocampal slices (Seese et al., 2012), which implicates microtubule-dependent mechanisms in replenishing the synaptic pool of cortactin. On the other hand, Shank1 may bind to deacetylated cortactin present in the synaptic pool, and acetylation of cortactin negatively modulates this interaction (Fig. 7C); indeed, whereas glutamate treatment promotes the dispersion of cortactin to dendritic shafts (Hering and Sheng, 2003), in agreement with its increased acetylation (Fig. 8D), Shank remains in the postsynaptic density after glutamate treatment (Hering and Sheng, 2003). It is possible that cortactin acetylation by inhibiting its binding to Shank promotes its translocation from spines to shafts. Therefore, we speculate that the decreased synaptic content of acetylated cortactin may result from an increased depletion (resulting from decreased interaction with Shank) of the synaptic pool of cortactin. Accordingly, the effect of cortactin acetylation on the dendritic clustering of PSD95 may be due to removal from the synapse of cortactin interacting partners that inhibit the clustering of PSD95.

The reversible acetylation status of cortactin provides a unique mechanism that regulates its F-actin binding activity (Zhang et al., 2007). We have now revealed an important role for cortactin acetylation in regulating synapse composition. What may be necessary for proper cortactin function is not so much a net change in serine or tyrosine phosphorylation or deacetylation/acetylation, but a continuous cycle of these processes allowing the dynamic regulation of the protein.

Materials and Methods

Antibodies and reagents

The following antibodies were used in this study: anti-PSD95 antibody from Affinity BioReagents (Golden, CO, USA) and from Cell Signaling Technology (Danvers, MA, USA); anti-GluA1 N-terminal antibody and anti-acetylated lysine antibody from Merck (Darmstadt, Germany) and sheep anti-GluA1 N-terminal

antibody (a kind gift from Dr Andrew Irving, University of Dundee, Scotland); anti-tubulin monoclonal, anti-acetylated tubulin monoclonal, anti-flag, and anti-actin antibodies (purchased from Sigma, Sintra, Portugal); anti-gephyrin antibody, anti-VGLUT1 antibody and anti-VGAT N-terminal antibody from Synaptic Systems (Goettingen, Germany); anti-p140Cap and anti-Src antibodies from Cell Signaling Technology (Danvers, MA, USA), anti-MAP2 and anti-synaptophysin antibodies from Abcam (Cambridge, UK); anti-acetylated cortactin (a kind gift from Dr Xiaohong Zhang, University of South Florida, Tampa, FL, USA); anti-cortactin and anti-pan Shank (1, 2 and 3) from Santa Cruz Biotechnology, Inc. (Santa Cruz, CA, USA) and anti-cortactin pY421 from Biosource-Invitrogen (Leiden, The Netherlands); anti-Shank1 antibody from UC Davis/NIH NeuroMab Facility (University of California, CA, USA); alkaline phosphatase-conjugated anti-rabbit and anti-mouse secondary antibodies from GE Healthcare (Carnaxide, Portugal); secondary fluorescent antibodies anti-rabbit Alexa 488 and Alexa 594, anti-sheep Alexa 568, anti-guinea pig Alexa 647, anti-mouse Alexa 647 and anti-mouse Texas Red (purchased from Molecular Probes, Leiden, The Netherlands) and secondary fluorescent antibody anti-chicken AMCA (purchased from Jackson ImmunoResearch, West Grove, PA, USA). Acti-Stain 555 Fluorescent Phalloidin was purchased from Cytoskeleton, Inc. (Denver, USA).

DNA constructs and primers

Cortactin-FLAG constructs were a kind gift from Dr Xiaohong Zhang (University of South Florida, Tampa, FL, USA). Cortactin shRNA resistant constructs were prepared with the QuikChange II XL-site-directed mutagenesis kit (Stratagene), using cortactin constructs as template and the primers 5′-tccaagcattgctcac-aagttgactcagtct-3′ and 5′-gactgagtcaacttgtgagcaatgcttgga-3′. For the generation of the short interfering RNA construct the DNA oligonucleotides 5′-gatcccc-gcactgctcacaagtggacttcaagagagtccacttgtgagcagtgctttttggaaa-3′ and 5′-agcttttccaa-aaagcactgctcacaagtggactctcttgaagtccacttgtgagcagtgcggg-3′ (corresponding to nucleotides 331–348 of the rat and mouse cortactin sequence) were annealed and subcloned into the *XhoI* and *Hpa*I sites of the pLentilox3.7 vector. The control shRNA targets firefly luciferase and was described previously (Flavell et al., 2006).

Hippocampal cultures

Cultures were prepared from hippocampal neurons using previously described methods (Goslin et al., 1998), with adaptations (Santos et al., 2012).

Subcellular fractionation

Synaptoneurosomes (SNSs) were prepared as previously described (Yin et al., 2002). The procedure for purification of postsynaptic density fractions (PSDs) was adapted from (Peça et al., 2011), as previously described (Santos et al., 2012).

Immunocytochemistry, microscopy and quantitative fluorescence analysis

Neurons were fixed for 10 min in 4% sucrose/4% paraformaldehyde in PBS, and permeabilized with PBS+0.25% Triton X-100 for 5 min at 4℃. The neurons were then incubated in 10% BSA in PBS for 30 min at 37℃ to block nonspecific staining, and incubated in appropriate primary antibody diluted in 3% BSA in PBS (2 h, 37℃). After washing, cells were incubated in secondary antibody diluted in 3% BSA in PBS (45 min, 37℃). The coverslips were mounted using fluorescent mounting medium from Dako (Glostrup, Denmark). Surface GluA1-containing receptors were stained as previously described (Santos et al., 2012). Imaging was performed on a Zeiss Axiovert 200 M microscope, using a 63×1.4 NA oil objective. Images were quantified using image analysis software (ImageJ). For quantitation, sets of cells were cultured and stained simultaneously, and imaged using identical settings. The protein signals were analyzed as described (Santos et al., 2012). Measurements were performed in three or four independent preparations, and at least 9 cells per condition were analyzed for each preparation. Statistical analysis was performed using unpaired Student's *t*-test or One way ANOVA followed by the Dunnett's test. For analysis of F-actin organization, hippocampal neurons, labeled with Acti-stain 555 phalloidin, were chosen by the GFP channel. F-actin clusters were defined operationally as 0.14–1.42 μm^2 F-actin-enriched puncta along dendrites (with an average pixel intensity at least 50% above that in the adjacent dendritic region). Eleven to fifteen neurons were selected for each experimental group, and three to four proximal dendrites per each neuron were analyzed.

Immunoprecipitation assays

Co-immunoprecipitation assays were performed using lysates of HEK 293FT cells transfected with the constructs of interest, as previously described (Santos et al., 2012).

Acknowledgements

We thank Susana R. dos Louros for the control-shRNA plasmid, Xiaohong Zhang (H. Lee Moffit Cancer Center and Research Institute, University of South Florida, FL, USA) for the cortactin constructs and for the anti-acetylated cortactin antibody, Carlo Sala (CNR Institute of Neuroscience, Milan, Italy) for the GFP-tagged Shank1 construct, Casper C. Hoogenraad (Utrecht University, The Netherlands) for the GFP-tagged p140Cap construct and Andrew Irving (University of Dundee, UK) for the anti-GluA1 N-terminus antibody. We also thank Elisabete Carvalho for assistance in the preparation of cultured hippocampal neurons.

Funding

Tatiana Catarino and Luís Ribeiro were supported by FCT, Portugal. This work was supported by FCT and FEDER, Portugal (PTDC/BIA-BCM/71789/2006 and PTDC/BIA-BCM/113738/2009).

Supplementary material available online at
http://jcs.biologists.org/lookup/suppl/doi:10.1242/jcs.110742/-/DC1

References

Allison, D. W., Chervin, A. S., Gelfand, V. I. and Craig, A. M. (2000). Postsynaptic scaffolds of excitatory and inhibitory synapses in hippocampal neurons: maintenance of core components independent of actin filaments and microtubules. *J. Neurosci.* **20**, 4545-4554.

Ammer, A. G. and Weed, S. A. (2008). Cortactin branches out: roles in regulating protrusive actin dynamics. *Cell Motil. Cytoskeleton* **65**, 687-707.

Caldeira, M. V., Melo, C. V., Pereira, D. B., Carvalho, R., Correia, S. S., Backos, D. S., Carvalho, A. L., Esteban, J. A. and Duarte, C. B. (2007). Brain-derived neurotrophic factor regulates the expression and synaptic delivery of alpha-amino-3-hydroxy-5-methyl-4-isoxazole propionic acid receptor subunits in hippocampal neurons. *J. Biol. Chem.* **282**, 12619-12628.

Carvalho, A. L., Caldeira, M. V., Santos, S. D. and Duarte, C. B. (2008). Role of the brain-derived neurotrophic factor at glutamatergic synapses. *Br. J. Pharmacol.* **153 Suppl. 1**, S310-S324.

Chwang, W. B., Arthur, J. S., Schumacher, A. and Sweatt, J. D. (2007). The nuclear kinase mitogen- and stress-activated protein kinase 1 regulates hippocampal chromatin remodeling in memory formation. *J. Neurosci.* **27**, 12732-12742.

Dent, E. W., Merriam, E. B. and Hu, X. (2011). The dynamic cytoskeleton: backbone of dendritic spine plasticity. *Curr. Opin. Neurobiol.* **21**, 175-181.

Fischer, A., Sananbenesi, F., Wang, X., Dobbin, M. and Tsai, L. H. (2007). Recovery of learning and memory is associated with chromatin remodelling. *Nature* **447**, 178-182.

Flavell, S. W., Cowan, C. W., Kim, T. K., Greer, P. L., Lin, Y., Paradis, S., Griffith, E. C., Hu, L. S., Chen, C. and Greenberg, M. E. (2006). Activity-dependent regulation of MEF2 transcription factors suppresses excitatory synapse number. *Science* **311**, 1008-1012.

Fontán-Lozano, A., Romero-Granados, R., Troncoso, J., Múnera, A., Delgado-García, J. M. and Carrión, A. M. (2008). Histone deacetylase inhibitors improve learning consolidation in young and in KA-induced-neurodegeneration and SAMP-8-mutant mice. *Mol. Cell. Neurosci.* **39**, 193-201.

Goslin, K., Asmussen, H. and Banker, G. (1998). *Culturing Nerve Cells*. Cambridge, MA: MIT Press.

Guan, J.-S., Haggarty, S. J., Giacometti, E., Dannenberg, J.-H., Joseph, N., Gao, J., Nieland, T. J. F., Zhou, Y., Wang, X., Mazitschek, R. et al. (2009). HDAC2 negatively regulates memory formation and synaptic plasticity. *Nature* **459**, 55-60.

Hering, H. and Sheng, M. (2003). Activity-dependent redistribution and essential role of cortactin in dendritic spine morphogenesis. *J. Neurosci.* **23**, 11759-11769.

Hu, X., Ballo, L., Pietila, L., Viesselmann, C., Ballweg, J., Lumbard, D., Stevenson, M., Merriam, E. and Dent, E. W. (2011). BDNF-induced increase of PSD-95 in dendritic spines requires dynamic microtubule invasions. *J. Neurosci.* **31**, 15597-15603.

Iki, J., Inoue, A., Bito, H. and Okabe, S. (2005). Bi-directional regulation of postsynaptic cortactin distribution by BDNF and NMDA receptor activity. *Eur. J. Neurosci.* **22**, 2985-2994.

Jaworski, J., Kapitein, L. C., Gouveia, S. M., Dortland, B. R., Wulf, P. S., Grigoriev, I., Camera, P., Spangler, S. A., Di Stefano, P., Demmers, J. et al. (2009). Dynamic microtubules regulate dendritic spine morphology and synaptic plasticity. *Neuron* **61**, 85-100.

Kim, M.-S., Akhtar, M. W., Adachi, M., Mahgoub, M., Bassel-Duby, R., Kavalali, E. T., Olson, E. N. and Monteggia, L. M. (2012). An essential role for histone deacetylase 4 in synaptic plasticity and memory formation. *J. Neurosci.* **32**, 10879-10886.

Kouzarides, T. (2000). Acetylation: a regulatory modification to rival phosphorylation? *EMBO J.* **19**, 1176-1179.

Kruchten, A. E., Krueger, E. W., Wang, Y. and McNiven, M. A. (2008). Distinct phospho-forms of cortactin differentially regulate actin polymerization and focal adhesions. *Am. J. Physiol. Cell Physiol.* **295**, C1113-C1122.

Levenson, J. M., O'Riordan, K. J., Brown, K. D., Trinh, M. A., Molfese, D. L. and Sweatt, J. D. (2004). Regulation of histone acetylation during memory formation in the hippocampus. *J. Biol. Chem.* **279**, 40545-40559.

Martinez-Quiles, N., Ho, H. Y., Kirschner, M. W., Ramesh, N. and Geha, R. S. (2004). Erk/Src phosphorylation of cortactin acts as a switch on-switch off

mechanism that controls its ability to activate N-WASP. *Mol. Cell. Biol.* **24**, 5269-5280.

Meiler, E., Nieto-Pelegrín, E. and Martinez-Quiles, N. (2012). Cortactin tyrosine phosphorylation promotes its deacetylation and inhibits cell spreading. *PLoS ONE* **7**, e33662.

Miller, C. A., Campbell, S. L. and Sweatt, J. D. (2008). DNA methylation and histone acetylation work in concert to regulate memory formation and synaptic plasticity. *Neurobiol. Learn. Mem.* **89**, 599-603.

Miśkiewicz, K., Jose, L. E., Bento-Abreu, A., Fislage, M., Taes, I., Kasprowicz, J., Swerts, J., Sigrist, S., Versées, W., Robberecht, W. et al. (2011). ELP3 controls active zone morphology by acetylating the ELKS family member Bruchpilot. *Neuron* **72**, 776-788.

Naisbitt, S., Kim, E., Tu, J. C., Xiao, B., Sala, C., Valtschanoff, J., Weinberg, R. J., Worley, P. F. and Sheng, M. (1999). Shank, a novel family of postsynaptic density proteins that binds to the NMDA receptor/PSD-95/GKAP complex and cortactin. *Neuron* **23**, 569-582.

Pang, P. T., Teng, H. K., Zaitsev, E., Woo, N. T., Sakata, K., Zhen, S., Teng, K. K., Yung, W. H., Hempstead, B. L. and Lu, B. (2004). Cleavage of proBDNF by tPA/plasmin is essential for long-term hippocampal plasticity. *Science* **306**, 487-491.

Peça, J., Feliciano, C., Ting, J. T., Wang, W., Wells, M. F., Venkatraman, T. N., Lascola, C. D., Fu, Z. and Feng, G. (2011). Shank3 mutant mice display autistic-like behaviours and striatal dysfunction. *Nature* **472**, 437-442.

Racz, B. and Weinberg, R. J. (2004). The subcellular organization of cortactin in hippocampus. *J. Neurosci.* **24**, 10310-10317.

Santos, S. D., Iuliano, O., Ribeiro, L., Veran, J., Ferreira, J. S., Rio, P., Mulle, C., Duarte, C. B. and Carvalho, A. L. (2012). Contactin-associated protein 1 (Caspr1) regulates the traffic and synaptic content of α-amino-3-hydroxy-5-methyl-4-isoxazolepropionic acid (AMPA)-type glutamate receptors. *J. Biol. Chem.* **287**, 6868-6877.

Seese, R. R., Babayan, A. H., Katz, A. M., Cox, C. D., Lauterborn, J. C., Lynch, G. and Gall, C. M. (2012). LTP induction translocates cortactin at distant synapses in wild-type but not Fmr1 knock-out mice. *J. Neurosci.* **32**, 7403-7413.

Sharma, S. K. (2010). Protein acetylation in synaptic plasticity and memory. *Neurosci. Biobehav. Rev.* **34**, 1234-1240.

Spange, S., Wagner, T., Heinzel, T. and Krämer, O. H. (2009). Acetylation of non-histone proteins modulates cellular signalling at multiple levels. *Int. J. Biochem. Cell Biol.* **41**, 185-198.

Stefanko, D. P., Barrett, R. M., Ly, A. R., Reolon, G. K. and Wood, M. A. (2009). Modulation of long-term memory for object recognition via HDAC inhibition. *Proc. Natl. Acad. Sci. USA* **106**, 9447-9452.

Tehrani, S., Tomasevic, N., Weed, S., Sakowicz, R. and Cooper, J. A. (2007). Src phosphorylation of cortactin enhances actin assembly. *Proc. Natl. Acad. Sci. USA* **104**, 11933-11938.

Vecsey, C. G., Hawk, J. D., Lattal, K. M., Stein, J. M., Fabian, S. A., Attner, M. A., Cabrera, S. M., McDonough, C. B., Brindle, P. K., Abel, T. et al. (2007). Histone deacetylase inhibitors enhance memory and synaptic plasticity via CREB:CBP-dependent transcriptional activation. *J. Neurosci.* **27**, 6128-6140.

Yang, X. J. and Seto, E. (2008). Lysine acetylation: codified crosstalk with other posttranslational modifications. *Mol. Cell* **31**, 449-461.

Yeh, S. H., Lin, C. H. and Gean, P. W. (2004). Acetylation of nuclear factor-kappaB in rat amygdala improves long-term but not short-term retention of fear memory. *Mol. Pharmacol.* **65**, 1286-1292.

Yin, Y., Edelman, G. M. and Vanderklish, P. W. (2002). The brain-derived neurotrophic factor enhances synthesis of Arc in synaptoneurosomes. *Proc. Natl. Acad. Sci. USA* **99**, 2368-2373.

Yoshii, A. and Constantine-Paton, M. (2007). BDNF induces transport of PSD-95 to dendrites through PI3K-AKT signaling after NMDA receptor activation. *Nat. Neurosci.* **10**, 702-711.

Zhang, X., Yuan, Z., Zhang, Y., Yong, S., Salas-Burgos, A., Koomen, J., Olashaw, N., Parsons, J. T., Yang, X.-J., Dent, S. R. et al. (2007). HDAC6 modulates cell motility by altering the acetylation level of cortactin. *Mol. Cell* **27**, 197-213.

Zhang, Y., Zhang, M., Dong, H., Yong, S., Li, X., Olashaw, N., Kruk, P. A., Cheng, J. Q., Bai, W., Chen, J. et al. (2009). Deacetylation of cortactin by SIRT1 promotes cell migration. *Oncogene* **28**, 445-460.